



HAL
open science

Electrochemical Filter To Remove Oxygen Interference Locally, Rapidly, and Temporarily for Sensing Applications

Mathieu Etienne, Thi Xuan Huong Le, Tauqir Nasir, Grégoire Herzog

► **To cite this version:**

Mathieu Etienne, Thi Xuan Huong Le, Tauqir Nasir, Grégoire Herzog. Electrochemical Filter To Remove Oxygen Interference Locally, Rapidly, and Temporarily for Sensing Applications. *Analytical Chemistry*, 2020, 92 (11), pp.7425-7429. 10.1021/acs.analchem.0c00395 . hal-02887147

HAL Id: hal-02887147

<https://hal.univ-lorraine.fr/hal-02887147v1>

Submitted on 1 Dec 2020

HAL is a multi-disciplinary open access archive for the deposit and dissemination of scientific research documents, whether they are published or not. The documents may come from teaching and research institutions in France or abroad, or from public or private research centers.

L'archive ouverte pluridisciplinaire **HAL**, est destinée au dépôt et à la diffusion de documents scientifiques de niveau recherche, publiés ou non, émanant des établissements d'enseignement et de recherche français ou étrangers, des laboratoires publics ou privés.



Distributed under a Creative Commons Attribution - NonCommercial - NoDerivatives 4.0
International License

An electrochemical filter to remove oxygen interference locally, rapidly and temporarily for sensing applications

Mathieu Etienne*, Thi Xuan Huong Le, Tauqir Nasir, Grégoire Herzog

Laboratoire de Chimie Physique et Microbiologie pour les Matériaux et l'Environnement,
UMR 7564, CNRS – Université de Lorraine, 405, rue de Vandoeuvre, F-54600 Villers-lès-
Nancy, France

* *Corresponding author:*

E-mail: mathieu.etienne@univ-lorraine.fr

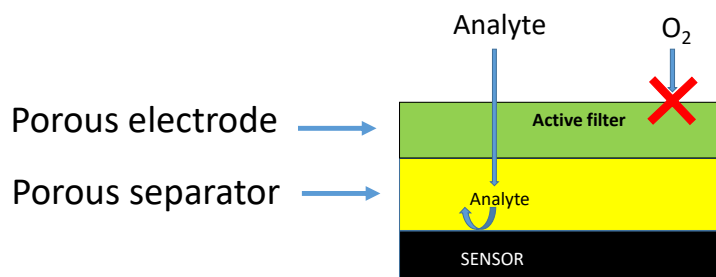
Tel.: +33 3 72 74 73 82; *Fax:* +33 (0)3 83 27 54 44

This document is a postprint. Final version has been published in *Analytical Chemistry* **2020**, *92*, 7425-7429 (<https://doi.org/10.1021/acs.analchem.0c00395>).

Abstract

An electrochemical oxygen filter is described that removes efficiently dissolved oxygen from the surface of an electrochemical sensor. Simulations show that 99 % of oxygen can be removed in less than 60 s if an electrochemical filter made of a porous electrode is positioned at less than 200 μm from the sensor surface. For experimental demonstration, the metallic filter was made with either a stainless steel or a platinum grids separated from the sensor by a porous separator. It was combined with a sensor for analysis of paraquat, an herbicide widely used over the world. In aerated solutions, paraquat signal was not distinguished due to the strong interference of oxygen. When using the oxygen filter, paraquat was clearly detected with a better-defined response than the one obtained under N_2 atmosphere that requires longer time before analysis.

Graphical abstract



KEYWORDS: oxygen interference, electrochemical sensor, electrochemical filter, paraquat, electroanalysis

1. Introduction

The detection of many analytes (N_2O ,^{1,2} NO_2^- ,³ NO_3^- ,⁴ CO_2 ,⁵ hydrazine,⁶ organic carbon content,⁷etc) is hindered by the presence of oxygen in the solution. A common method to eliminate dissolved oxygen in laboratory experiments is the purge of the solution with an inert gas such as nitrogen or argon. However, this method is time consuming if reaching a very low concentration of oxygen is required, is not necessarily reproducible if a shorter time of purge is used, and is not suitable for out-of-the-laboratory measurements.

For sensing applications, oxygen scavengers have been tested for several analytes. For example, phosphines¹ and ascorbic acid⁸ can consume oxygen in N_2O sensors and sodium thiosulfate was applied to H_2O_2 sensing.⁹ Pluméré *et al.* proposed an enzymatic oxygen scavenger using glucose, galactose or pyranose 2-oxidase as effective catalysts for O_2 reduction⁴ and the efficiency of the system was evaluated for the biosensing of nitrate. More recently, enzyme immobilization in a thin polymeric film at the surface of the electrode suppressed the need to introduce the enzyme in the whole solution, but one still needs to

introduce in the whole volume the aldohexose substrate that will react with oxygen and this is the main drawback of oxygen scavengers.¹⁰

Another solution is provided by electrochemical methods. Porous silver electrodes were initially used to remove oxygen in the solution of analysis.¹¹ Different configurations and electrode materials have been proposed to reach the complete oxygen removal for analytical or other purposes.^{7,12-14} Drawbacks of such approaches are the production of H₂O₂ or the alteration of pH due to a quantitative conversion of oxygen initially present in the treated solution.¹⁴ Miniaturization has been described, using two gold porous electrodes in a glass micro-capillary to remove oxygen interfering with N₂O detection,² and application of electrochemical dissolved oxygen removal from microfluidic streams was also shown.¹⁵ Finally, a sandwich electrode was evaluated for multi-gas analysis.¹⁶ In that case, oxygen interference could be significantly decreased but not totally suppressed.

Electrochemistry is powerful to remove oxygen on demand, but it is preferential to restrict the removal of oxygen to a limited volume near the surface of the sensor, without affecting significantly oxygen concentration in the whole volume of the analyte solution. For that purpose, interdigitated electrodes has been reported for oxygen removal in N₂H₄ sensors, but only 80% of oxygen molecules was prevented from reaching the sensing electrode.⁶ Of related interest, a thin layer of redox polymer was deposited on electrode with embedded redox proteins to provide a full electrochemical protection for oxygen sensitive , by reacting locally with oxygen at the electrode surface before it reaches the sensitive catalytic site of the enzyme.¹⁷ So, it is possible to reach complete oxygen removal, locally, with electrochemical methods if a suitable system architecture is proposed.

Our goal here was thus to remove oxygen only from the surface of an electrochemical sensor, and not from the all solution. The expected advantages are a rapid (within a minute) and reproducible removal of oxygen, and a design that could be easily implemented in commercial

sensor platforms. We first conducted simulation of ideal electrochemical cells, with a grid electrode as oxygen filter and a sensor as second working electrode, the two electrodes being separated by a controlled distance. Later, we implemented the system experimentally using platinum or stainless steel grids as electrochemical oxygen filter and a porous layer to separate the sensor from the filter. At first, experiments have been conducted to demonstrate the local oxygen removal and finally, we evaluated the performance of this electrochemical filter for eliminating oxygen from the surface of a sensor for paraquat, a pesticide, which detection is very sensitive to oxygen traces.¹⁸

2. Experimental section

2.1. Materials

Stainless steel (SS, 0.103 nominal aperture, 0.066 mm wire diameter) and Platinum (Pt, 0.12 mm nominal aperture, 0.04 wire diameter) grids were purchased from Goodfellow SARL with purity of 99.9 %. Porous filters (DVPP), glassy carbon electrode (GCE) were bought from Merck Milipore and Sigradur HTWHochtemperatur-Werkstoffe, Germany, respectively. Potassium chloride (KCl), hydrogen peroxide (H₂O₂), paraquat, were obtained from Sigma-Aldrich and sodium nitrate (NaNO₃) from Prolabo. These chemicals were used without any further purification. All solutions were prepared with high purity water (18 MΩ cm) from a Purelab Option water purification system (Elga LabWater, Veolia Water STI, France).

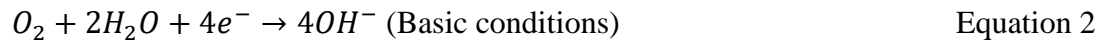
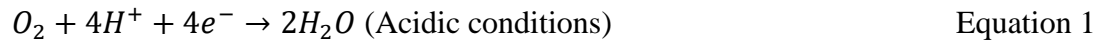
2.2. Electrochemical experiments

The electrochemical cell was composed of four electrodes and fabricated from Teflon. The glassy carbon electrode (working electrode 1) and the metallic filter (working electrode 2) were separated by a porous layer with diameter of 0.5 cm and pore size at 0.65 μm. Glassy carbon was firstly wet-polished by SiC grinding paper (#4000, Struers, Denmark) for 1 min, then cleaned with ethanol and distilled water under ultrasonic condition. The experiments were conducted with on a Palm Sens 3 potentiostat in a four-electrode configuration (two working

electrodes, Ag/AgCl/3M KCl reference electrode, and stainless steel counter electrode). The reaction of oxygen with the filter and the efficiency of the electrochemical removal was characterized by cyclic voltammetry. Usually, a 10 mL aqueous solution of KCl (0.1 M) was utilized as supporting electrolyte. When needed, purging the solution with N₂ gas was performed at least 15 min before running experiment and N₂ flow kept over the solution during the experiment. The modification of glassy carbon with mesoporous silica was achieved by sol-gel electrodeposition following strictly a protocol recently reported.¹⁸ Paraquat detection have been performed in 0.07 M NaNO₃ as it was optimized previously.¹⁸

2.3. Theory and Methodology

We simulated the reduction of dissolved oxygen (Equations 1 & 2) at the surface an electrochemical filter and monitored the variation of its concentration within an electrochemical cell and in the vicinity of a sensor located at the bottom of the electrochemical cell (Figure 1A).



The electrochemical cell is described as a cylinder of a radius r_{cell} of 2.5 mm and a height h_{cell} of 6 mm. The working disk electrode used as a sensor is located at the bottom of the electrochemical cell ($z = 0$) and is of the same diameter as the electrochemical cell. A porous layer is placed on top of the disk working electrode, with a thickness of $h_{porous\ layer} = 125\ \mu\text{m}$ and a porosity, P , of 0.7. The electrochemical filter is a Pt mesh made of intertwined wires of varied radii (25, 50, 100 μm spaced respectively by 100, 200, and 400 μm) and located at varied distances from the sensor ($z = 150, 175, 200, 250, 275, 325\ \mu\text{m}$).

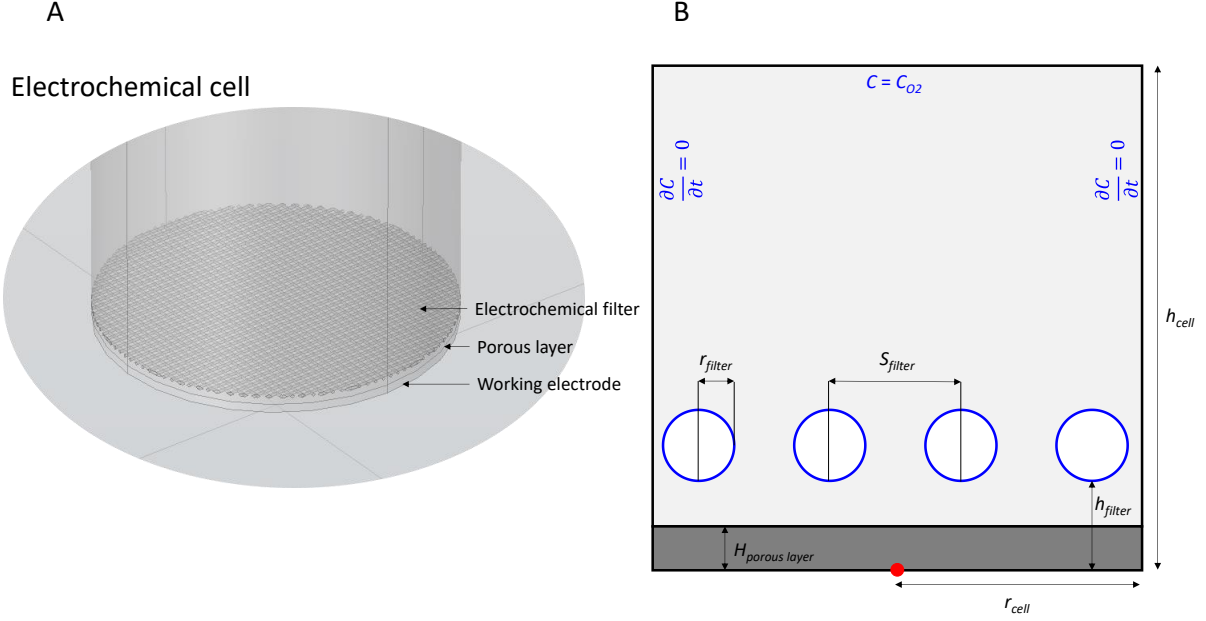


Figure 1. (A) 3D representation of the electrochemical cell. (B) 2D representation of the electrochemical cell with the definition of the cell parameters (in black) and of the boundary conditions (in blue). The blue circles represent the Pt wires of the electrochemical wires at which the dissolved oxygen is reduced. The red point is the position at which the dissolved oxygen concentration is calculated (i.e., the surface of the sensor that is associated with this filter).

Transport of species is considered by diffusion only, described by a time-dependent diffusion equation in Cartesian coordinates (Equation 3).

$$\frac{\partial C}{\partial t} = D \left(\frac{\partial^2 C}{\partial x^2} + \frac{\partial^2 C}{\partial y^2} + \frac{\partial^2 C}{\partial z^2} \right) \quad \text{Equation 3}$$

C is the concentration, t is the time, D is the diffusion coefficient. The working disk electrode is separated from the electrochemical filter by a porous insulating layer of porosity P . The diffusion coefficient for dissolved oxygen in the membrane, $D_{porous\ layer}$ is given by equation 4:

$$D_{porous\ layer} = P \times D_{cell} \quad \text{Equation 4}$$

Simulations were run on a simplified 2D projection of the electrochemical cell (Figure 1B), where boundary conditions are shown for the domain studied. For all simulations, the potential of the sensor electrode was kept at open-circuit potential.

2.5. Computational details

Simulations were performed using the finite element method program package COMSOL Multiphysics (version 5.4, COMSOL Ltd, Hertfordshire, United Kingdom) equipped with the electrochemistry module. Free mesh parameters were used at locations where high concentration gradients occur, i.e. around the electrochemical filter, at the boundary between the electrochemical cell and the porous layer. The maximum size of the triangular elements of 0.0008 and a factor of 1.2 for element expansion were used. The PARDISO linear solver was used, with an absolute tolerance of 0.1 and a relative tolerance of 0.001. The parameters used for all simulations are gathered in Table S1 in Supporting Information.

Results and discussion

Modeling of oxygen concentration profiles

Influence of the wire diameter of the electrochemical filter

After validating the simulation program (see Figure S1), we investigated the concentration profile for dissolved oxygen using three different kinds of electrochemical filters. The size of the platinum mesh was varied with three different wire radii (25, 50, and 100 μm). The spacing between wires was adjusted (100, 200, 400 μm) to maintain the ratio $S_{\text{filter}} / r_{\text{filter}}$ constant at 4. The distance between the electrochemical filter and the electrode, h_{filter} , was kept constant at 225 μm . For these three electrochemical filters, the variation of the dissolved oxygen concentration, at the sensor surface, over time was simulated for a potential applied of $E_0 - 0.5$ V (Figure 2A). In order to compare the dissolved consumption at the vicinity of the sensor, we compared the time necessary for the concentration to drop below 1 % of the initial concentration C_{O_2} , $t_{1\%}$. For the smaller mesh, $t_{1\%}$ was of 67 s, while 86 s were necessary for the intermediate mesh and 200 s for the largest. These results are expected as a smaller mesh will have the highest electroactive surface area and indeed will allow faster depletion of the zone between the electrochemical filter and the sensor.

Influence of the electrochemical filter – electrode distance

The influence of the distance between the electrochemical filter and the working electrode, h_{filter} , on $t_{1\%}$ is now investigated (Figure 2B). The h_{filter} value was varied between 125 and 225 μm . The lowest value is limited by the thickness of the porous layer, acting as an electric insulator between the electrochemical filter and the working electrode. The value of $t_{1\%}$ decreased with the distance between the electrochemical filter and the working electrode.

These simulations show that the presence of dissolved oxygen in the vicinity of the working electrode can be reduced to less than 1 % of the original value within less than a minute, which constitutes an advantage over N_2 purging. The use of the electrochemical filter is a time gain and simplifies the electrochemical set-up in the view of on-site analysis.

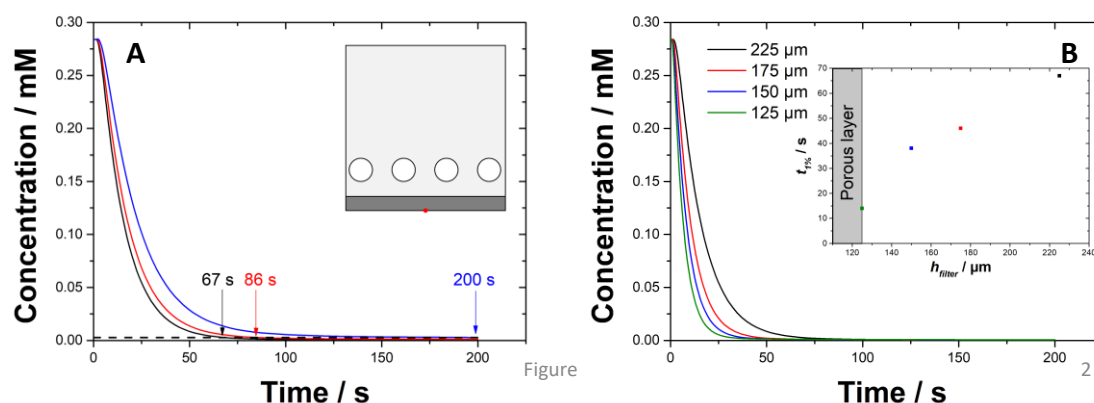


Figure 2. (A) Variation of the dissolved oxygen concentration over time for different electrochemical filters; concentrations are shown for the point marked as a red dot on the inset. Electrochemical filters: (**black**) $r_{wire} = 25 \mu\text{m}$, $S_{filter} = 100 \mu\text{m}$, $h_{filter} = 225 \mu\text{m}$; (**red**) $r_{wire} = 50 \mu\text{m}$, $S_{filter} = 200 \mu\text{m}$, $h_{filter} = 225 \mu\text{m}$; (**blue**) $r_{wire} = 100 \mu\text{m}$, $S_{filter} = 400 \mu\text{m}$, $h_{filter} = 225 \mu\text{m}$. The dash line represents the 1 % of the initial concentration and the time values given are the $t_{1\%}$ (i.e. the time necessary for the concentration to reach 1 % of the initial concentration). (B) Variation of the dissolved oxygen concentration over time for an electrochemical filter located at various distances from the sensor electrode. Electrochemical filter: $r_{wire} = 25 \mu\text{m}$, $S_{filter} = 100 \mu\text{m}$, $h_{filter} = 225 \mu\text{m}$ (black), 175 μm (red), 150 μm (blue), and 125 μm (green). Concentrations are shown for the point marked as a red dot on the inset of Figure 2A. Inset: $t_{1\%}$ values for the different h_{filter} distances.

Experimental validation

For experimental validation, we tested platinum and stainless grids as oxygen filter. The porous layer was a filtration membrane. A schematic of the experimental setup is provided in Figure S2 in SI. The sensor and the metallic filter sandwiched the porous layer, in contact with each other in order to reach the more rapid deoxygenation (see modeling section). Working electrodes were connected to a bipotentiostat in a four-electrode configuration, including a reference electrode and a counter electrode.

Figure 3A shows the electrochemical reduction of dissolved oxygen on a platinum filter (curve a) and stainless steel (curve b). Oxygen reduction occurs at -0.360 V on platinum and about -0.575 V on stainless steel (half-wave potentials). This means that it is necessary to apply a more negative potential on stainless steel than on platinum to remove efficiently oxygen. Because platinum is a good material for catalytic reduction of oxygen, its better behaviour than stainless steel is expected. However, if one considers the cost criteria, the steel material is much cheaper and could thus be a suitable option.

We first evaluated the stainless steel grid by performing several cycles of deoxygenation/oxygenation. Oxygen was detected on glassy carbon electrode used here as oxygen sensor (Figure 3B, curve a). A potential of -0.7 V was applied to the stainless steel filter in order to perform oxygen reduction and indeed, this potential permitted a complete removal of oxygen from the sensor surface (curve b of Figure 3B). Oxygenation of the solution was achieved by stirring with a magnetic bar positioned 5 mm away from the sensor. Almost immediately, the oxygen was introduced back on the surface of the sensor that could be detected up to five times. After each oxygenation step, the application of -0.7 V to the oxygen filter allowed the rapid removal of oxygen from the sensor surface (see Figure S3 in SI). We also validated the platinum grid as filter (see Figure S4 in SI). The main advantage of platinum is that potential applied to the filter can be less negative, being efficient at -0.4 V.

Electrochemical sensing of paraquat using designed electrochemistry cell

Paraquat, a chemical compound highly soluble in water, is used as herbicide to control broad leaf weeds in agricultural practices since the early 1960s.¹⁹ It is used worldwide in more than 100 countries but is banned in European Union. It causes severe toxicity to living organisms by damaging the lungs, kidneys, liver and heart.²⁰ The main route of paraquat toxicity is oral and it then circulates to other organs by blood stream leading to multiple organ failure and ultimately death.²¹ It is also reported to cause Parkinson's disease.²² Therefore, it is necessary to detect this compound at small concentration in aqueous medium. At low concentration, paraquat can be detected by electrochemical methods.

Electrochemically speaking, paraquat is methyl viologen (1,1'-dimethyl-4,4'-bipyridinium). It can be reduced to two successive one electron reactions at -0.7 V and -1.025 V²³ and then oxidized back to the relative potential values. For electrochemical sensing of paraquat, study of the first redox reaction is sufficient for quantification of paraquat in the aqueous media.²⁴ This was recently illustrated by Tauqir *et al.* that developed a paraquat sensor based on glassy carbon electrodes modified with thin mesoporous silica films.¹⁸ We used this sensor to illustrate the performance of the electrochemical oxygen filter.

A main issue with paraquat is that the electrochemical detection is not possible in the presence of dissolved oxygen. The accuracy of the analysis depends on a deoxygenation of the solution. This problem is illustrated in Figure 3C. Curve a reports the electrochemical detection of paraquat in the presence of oxygen. A large cathodic signal is observed, which is the overlay of the reduction of both 20 μM paraquat and dissolved oxygen reduction, the latter reacting directly on the sensor surface or with the reduced form of paraquat itself. The application of -0.5 V at a platinum filter leads to dramatic decrease of the current (curve b of Figure 3C). With the electrochemical filter, the cyclic voltammetry of paraquat is well defined (curve b of Figure 3D for a detailed view) and the presence of oxygen is unnoticeable. This signal is reproducible

over multiple CV detections ($I_{\text{cathodic}}=0.59\pm 0.02 \mu\text{A}$, $N=3$, see Figure S5). On the contrary, when the detection of paraquat has been performed by removing O_2 by bubbling N_2 for 15 min, a slight distortion of the cyclic voltammetric signal was observed, leading to higher cathodic current (curve a of Figure 3D). We attribute this phenomenon to trace of oxygen still present in the sample to analyze. Of course, longer N_2 bubbling would have allowed the removal of this residual oxygen concentration, but this experiment showed precisely the advantage of the electrochemical filter for sensing application. As suggested by simulation, the residual concentration of oxygen is low enough within a few minutes to allow electrochemical analysis whereas much longer time is required for the removal of oxygen by an inert gas.

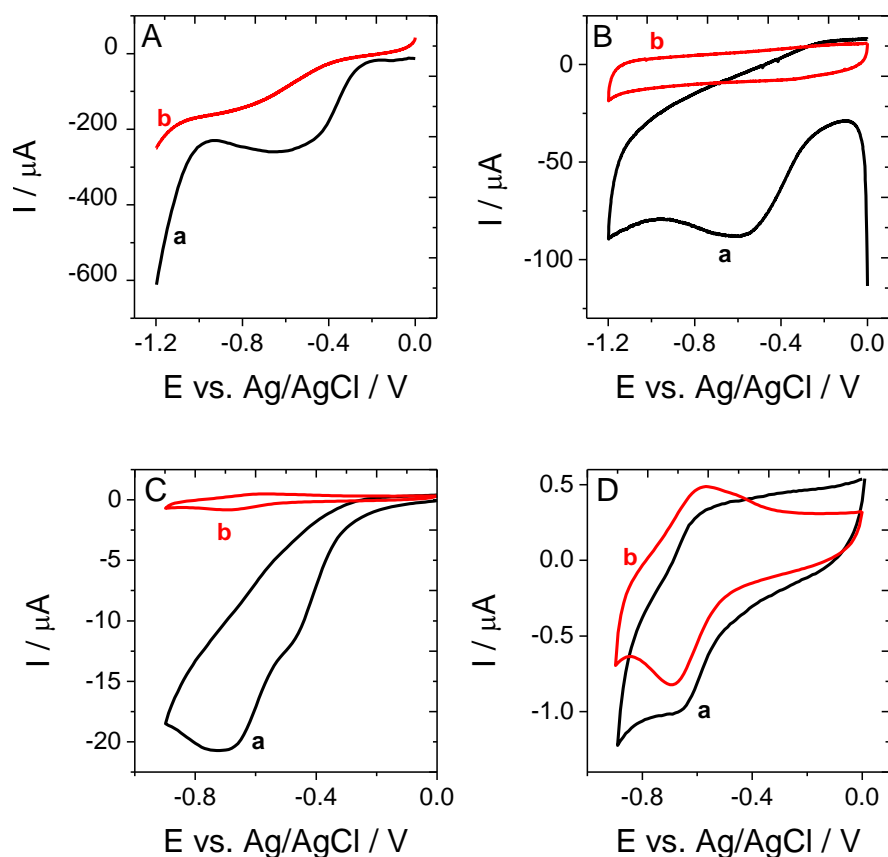


Figure 3. (A) Linear sweep voltammetric response in aerated 0.1 M KCl solution of (a) a platinum filter and (b) a stainless steel filter (scan rate: 100 mV s^{-1}). (B) Cyclic voltammetric responses in aerated 0.1 M KCl solution of a glassy carbon electrode (a) before and (b) 5 min after activation of the oxygen filter by applying -0.7 V at a stainless steel filter (scan rate: 100 mV s^{-1}). (C) Cyclic voltammetric responses to $20 \mu\text{M}$ paraquat in 0.07 M NaNO_3 aerated

solution at silica thin film modified GCE (a) without and (b) with local oxygen removal by applying -0.5 V vs. Ag/AgCl at a platinum filter for 5 min. **(D)** Similar experimental conditions, to compare the CV responses to 20 μM paraquat (a) with 15 min N_2 purge and (b) with oxygen removal by applying -0.5 V at a platinum filter for 5 min. Scan rate for C&D: 20 mV s^{-1} .

As the advantages of the method have been discussed (local and rapid removal of oxygen, possibility to alternate activation and inactivation of the filter), the potential drawbacks must be also considered carefully. The first one, the most important, is related to pH. First estimations made with an initial pH of 7 shows that indeed, pH can change dramatically from 7 to 11 at the sensor surface when oxygen is ideally reduced to water, but this variation can also be minimized with a low concentration pH buffer, i.e. 5 to 10 mM phosphate buffer (see Figure S6 and the associated discussion). The second one is the generation of reactive oxygen species (ROS) at the filter while oxygen is reduced. ROS could damage sensor surface or affect the analyte and great attention should be paid to this issue. However, many electrochemical sensors are of single-use and the possibility to activate/inactivate the oxygen filter will limit this production of ROS. No evidence of detrimental influence of ROS was noticed up to now. The third one is related to the limited number of target analytes that would be both sensitive to oxygen but not reduced at the same potential as oxygen on the filter. Apart viologen, important molecules are concerned, such as the oxidized form of nicotinamide adenine dinucleotide (NAD^+) and nitrogen species (NO_3^- , NO_2^- , N_2O). Moreover, a different detection scheme could be considered, such as anodic stripping detection of heavy metals sensitive to oxygen (Cd, Pb and Zn), taking advantage of the sequential control of the filter activity.

4. Conclusion

An electrochemical filter has been designed to perform oxygen removal in the vicinity of sensor surface. The initial modelling has shown that the deoxygenation could be reached

rapidly, in the range of a minute if a porous electrode was positioned close enough from the sensor surface. Experimentally, we demonstrated that stainless steel and platinum grids could remove oxygen efficiently, no oxygen was detected by the sensor, and repeatedly. The device was combined with a paraquat sensor and show good performances regarding the elimination of oxygen interference: no oxygen was observed when the platinum filter was switched on at -0.5 V for 5 minutes, much better than after 15 min N₂ bubbling for which a trace of oxygen was still detected. The next step of this research is the combination of the electrochemical filter with screen printed sensors commercially available for the detection of other species sensitive to oxygen, such as nitrogen species, some heavy metals (Cd, Pb, Zn) or biomolecules (for example, NAD⁺ cofactor). Moreover, some issues remain and are worth of investigating such as the dissolved oxygen concentration that we need to go for environmental applications, the consequence of a local variation of pH and local production of reactive oxygen species at the surface of the sensor, and the effect of convection on the efficiency of the local electrochemical filter.

Supporting Information. Simulations parameters, simulation for program validation, schematic of the experimental setup, additional electrochemical experiments to support the discussion.

Acknowledgements

This work was supported partly by the French PIA project « Lorraine Université d'Excellence », reference ANR-15-IDEX-04-LUE. TN is grateful to the Higher Education of Pakistan for funding his PhD.

References

- (1) Sveegaard, S. G.; Nielsen, M.; Andersen, M. H.; Gothelf, K. V. Phosphines as Efficient Dioxygen Scavengers in Nitrous Oxide Sensors. *ACS Sensors* **2017**, *2*, 695–702.
- (2) Revsbech, N. P.; Nielsen, L. P.; Christensen, P. B.; Sørensen, J. Combined Oxygen and Nitrous Oxide Microsensor for Denitrification Studies. *Appl. Environ. Microbiol.* **1988**, *54*, 2245–229.
- (3) Plumeré, N. Interferences from Oxygen Reduction Reactions in Bioelectroanalytical Measurements: The Case Study of Nitrate and Nitrite Biosensors. *Anal. Bioanal. Chem.* **2013**, *405*, 3731–3738.
- (4) Plumeré, N.; Henig, J.; Campbell, W. H. Enzyme-Catalyzed O₂ Removal System for Electrochemical Analysis under Ambient Air: Application in an Amperometric Nitrate Biosensor. *Anal. Chem.* **2012**, *84*, 2141–2146.
- (5) Qian, F.; Lu, J.; Zhou, Z.; Cha, C. Combined Amperometric Sensors for Simultaneous Measurement of Carbon Dioxide and Oxygen. *Sensors Actuators B Chem.* **1993**, *17*, 77–83.
- (6) Bertin, E.; Garbarino, S.; Guay, D. Interdigitated Microelectrodes for Oxygen Removal in N₂H₄ Sensors. *Electrochem. commun.* **2016**, *71*, 56–60.
- (7) Quek, S. B.; Cheng, L.; Cord-Ruwisch, R. In-Line Deoxygenation for Organic Carbon Detections in Seawater Using a Marine Microbial Fuel Cell-Biosensor. *Bioresour. Technol.* **2015**, *182*, 34–40.
- (8) Andersen, K.; Kjar, T.; Revsbech, N. P. An Oxygen Insensitive Microsensor for Nitrous Oxide. *Sensors Actuators, B Chem.* **2001**, *81*, 42–48.
- (9) Gu, Y.; Chen, C. C. Eliminating the Interference of Oxygen for Sensing Hydrogen Peroxide with the Polyaniline Modified Electrode. *Sensors* **2008**, *8*, 8237–8247.
- (10) Conzuelo, F.; Schuhmann, W.; Marković, N.; Zacarias, S.; Pereira, I. A. C.; Ruff, A.; Szczesny, J.; Lubitz, W. A Fully Protected Hydrogenase/Polymer-Based Bioanode for

- High-Performance Hydrogen/Glucose Biofuel Cells. *Nat. Commun.* **2018**, *9*, 3675.
- (11) Hanekamp, H. B.; Voogt, W. H.; Bos, P.; Frei, R. W. An Electrochemical Scrubber for the Elimination of Eluent Background Effects in Polarographic Flow-through Detection. *Anal. Chim. Acta* **1980**, *118*, 81–86.
- (12) Vuorilehto, K.; Tamminen, A.; Yläsaari, S. Electrochemical Removal of Dissolved Oxygen from Water. *J. Appl. Electrochem.* **1995**, *25*, 973–977.
- (13) Tamminen, A.; Vuorilehto, K.; Yläsaari, S. Scale-up of an Electrochemical Cell for Oxygen Removal from Water. *J. Appl. Electrochem.* **1996**, *26*, 113–117.
- (14) Holubowitch, N. E.; Omosebi, A.; Gao, X.; Landon, J.; Liu, K. Membrane-Free Electrochemical Deoxygenation of Aqueous Solutions Using Symmetric Activated Carbon Electrodes in Flow-through Cells. *Electrochim. Acta* **2019**, *297*, 163–172.
- (15) Marei, M. M.; Roussel, T. J.; Keynton, R. S.; Baldwin, R. P. Electrochemical Dissolved Oxygen Removal from Microfluidic Streams for LOC Sample Pretreatment. *Anal. Chem.* **2014**, *86*, 8541–8546.
- (16) Hahn, C. E. W.; Hall, E. A. H.; Maynard, P.; Albery, W. J. A Sandwich Electrode for Multi-Gas Analysis: A Prototype. *Br. J. Anaesth.* **1982**, *54*, 681–687.
- (17) Plumeré, N.; Rüdiger, O.; Oughli, A. A.; Williams, R.; Vivekananthan, J.; Pöller, S.; Schuhmann, W.; Lubitz, W. A Redox Hydrogel Protects Hydrogenase from High-Potential Deactivation and Oxygen Damage. *Nat. Chem.* **2014**, *6*, 822–827.
- (18) Nasir, T.; Herzog, G.; Hébrant, M.; Despas, C.; Liu, L.; Walcarius, A. Mesoporous Silica Thin Films for Improved Electrochemical Detection of Paraquat. *ACS Sensors* **2018**, *3*, 484–493.
- (19) Sagar, G. R. Uses and Usefulness of Paraquat. *Hum. Exp. Toxicol.* **1987**, *6*, 7–11.
- (20) Gao, R.; Choi, N.; Chang, S. I.; Kang, S. H.; Song, J. M.; Cho, S. I.; Lim, D. W.; Choo, J. Highly Sensitive Trace Analysis of Paraquat Using a Surface-Enhanced Raman

- Scattering Microdroplet Sensor. *Anal. Chim. Acta* **2010**, *681*, 87–91.
- (21) Senarathna, L.; Eddleston, M.; Wilks, M. F.; Woollen, B. H.; Tomenson, J. A.; Roberts, D. M.; Buckley, N. A. Prediction of Outcome after Paraquat Poisoning by Measurement of the Plasma Paraquat Concentration. *Qjm* **2009**, *102*, 251–259.
- (22) Tanner, C. M.; Kame, F.; Ross, G. W.; Hoppin, J. A.; Goldman, S. M.; Korell, M.; Marras, C.; Bhudhikanok, G. S.; Kasten, M.; Chade, A. R.; Comyns, K.; Richards, M. B.; Meng, C.; Priestley, B.; Fernandez, H. H.; Cambi, F.; Umbach, D. M.; Blair, A.; Sandler, D. P.; Langston, J. W. Rotenone, Paraquat, and Parkinson's Disease. *Environ. Health Perspect.* **2011**, *119*, 866–872.
- (23) Bird, C. L.; Kuhn, A. T. Electrochemistry of the Viologens. *Chem. Soc. Rev.* **1981**, *10*, 49–82.
- (24) Zen, J. M.; Jeng, S. H.; Chen, H. J. Determination of Paraquat by Square-Wave Voltammetry at a Perfluorosulfonated Ionomer/Clay-Modified Electrode. *Anal. Chem.* **1996**, *68*, 498–502.